Aging in the ferroic random-field Ising model system strontium-barium niobate

S. Miga,[1,2] J. Dec,[1,2] W. Kleemann,[1] and R. Pankrath[3]
[1]*Angewandte Physik, Universität Duisburg-Essen, D-47048 Duisburg, Germany*
[2]*Insitute of Physics, University of Silesia, Pl-40-007 Katowice, Poland*
[3]*Fachbereich Physik, Universität Osnabrück, D-46069 Osnabrück, Germany*
(Received 20 April 2004; published 25 October 2004)

Large aging effects, investigated via temporal dependences of the dielectric response, are found to be inherent in the uniaxial ferroelectric relaxor systems SBN:Cr and SBN:Ce. The results are discussed on the basis of domain coarsening and domain-wall pinning effects. Owing to the different charge disorder induced by the Cr^{3+} and Ce^{3+} dopants, a fundamental difference between both systems is established. While SBN:Ce shows only a weak breaking of ergodicity, the SBN:Cr system experiences true ergodicity breaking.

DOI: 10.1103/PhysRevB.70.134108 PACS number(s): 77.80.−e, 64.60.My, 77.84.Dy

I. INTRODUCTION

Ferroelectric relaxors as disordered systems have been intensively studied as very promising materials in many fields of application.[1] In this context the temporal stability of useful properties of practical devices is of primary importance. Since aging is a phenomenon that manifests itself through the dependence of the properties of a given material on the history of the specimen,[2] it must be thoroughly explored before making use of the selected material in applications. Likewise, such studies also have a considerable scientific significance because physical systems with extremely slow relaxation dynamics are, at the same time, ubiquitous and very fascinating subjects for fundamental research.[3] In this meaning, aging reflects the fact that the time needed for the system to be equilibrated becomes much larger than the experimental time scale.[2]

The key issue of relaxors is the appearance of polar clusters in the paraelectric phase,[4,5] which are correlated by the fluctuations of relatively weak random fields (RFs).[6–8] In cubic relaxors, like lead magnoniobate (PMN) with almost continuous order parameter ($n=8$ easy directions along $\langle 111 \rangle$), the dipolar interaction between the polar clusters is proposed to be at the origin of a random-bond, random-field-dominated glassy transition.[9] Hence, a cluster glass defines the ground state of PMN at $T<T_c$. On the other hand, the open tetragonal tungsten bronze-type strontium-barium niobate, $Sr_{0.61}Ba_{0.39}Nb_2O_6$ (SBN), has a one-component order parameter, which, in the presence of immobile electric monopoles, makes the system a candidate for the $3d$ random-field Ising model (RFIM) universality class.[10,11] Consequently, the polar clusters freeze into a metastable domain state at $T<T_c$, rather than into a cluster glass. Such nanodomains with a fractal size distribution have been directly observed using high-resolution piezoresponse microscopy.[12] Metastability in domains and domain wall configurations causes the structure to be subject to a very slow "aging" dynamics driving it gradually towards equilibrium.

Several models for aging and related phenomena, such as rejuvenation and memory,[2,13,14] have already been proposed and can be subdivided in two main categories.[15] On one hand, the phase-space picture originating from mean-field theory suggests a hierarchical arrangement of numerous metastable states. Here, aging of a given system is pictured as a random walk among these metastable states,[15] which gradually finds a lower free-energy state, when allowed to reside under fixed conditions.[14] Due to the existence of significant barriers in the energy landscape, it is difficult for the system to visit the whole phase space very quickly.[13] Since no breaking of chemical bonds is involved, such a slow relaxation process is often denoted as a *physical* aging.[13] On the other hand, real-space droplet or domain models have been developed for spin glasses or disordered ferroelectrics, respectively. In the latter case, aging can be understood from the dynamics of pinned domain walls and domain coarsening effects: as time elapses, the density of movable domain walls decreases, and the remaining domain walls are better and better pinned. This process manifests itself in a gradual decrease of susceptibility.[13,14,16]

It is believed that depending on the complexity of the system, different aging scenarios can be manifested. While aging due to a simple growth of domains is typically cumulative, in contrast, aging of a spin glass at one designated temperature, T_a, has little effect on the dielectric susceptibility $\chi(T)$ at lower temperature, $T<T_a$. It creates a long-term memorized hole-type aging that can be read out in $\chi(T)$ later upon subsequent warming up to $T>T_a$.[14] The most important goal of this paper is to recognize the aging scenario in Ce^{3+} and Cr^{3+} doped SBN single crystals as a newly established RFIM.[11] These two different trivalent cations are known to replace A and B sites,[17,18] respectively, in the crystal structure referring to the general formula AB_2O_6, and thus give rise to different quenched charge disorder[11] owing to the replacement of bivalent and pentavalent main constituent ions, respectively.[17] We will concentrate on the temperature range just adjacent to T_c, since in the deep ferroelectric state at $T \ll T_c$, the aging of La-doped SBN has already been identified as a purely cumulative one, thus being in sharp contrast to the data from the lead-based PMN relaxor.[14] On the other hand, at $T<T_c$ the RF-controlled domains are expected to relax slowly towards long-range order.[19] This specific feature should particularly reveal itself in the hertz and subhertz frequency ranges of the probing ac electric field.

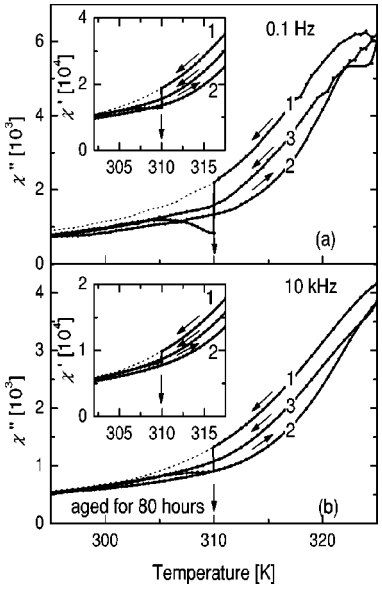

FIG. 1. Aging of the susceptibility components χ'' (main panels) and χ' (insets) of SBN:Cr measured vs temperature after ZFC from $T=450$ K at rates $\dot{T}=\mp 0.016$ Ks^{-1} and frequencies 10^{-1} Hz (a) and 10^4 Hz (b) on first cooling to 290 K with intermittent halt (80 h) at 310 K (curve 1), reheating to 325 K (curve 2), and subsequent continuous cooling back to 290 K (curve 3).

II. EXPERIMENTAL DETAILS

Congruently melting SBN crystals doped with Ce and Cr [$Sr_{0.61-x}Ce_xBa_{0.39}Nb_2O_6$, $x=0.0066$, SBN:Ce; $Sr_{0.61}Ba_{0.39}(Nb_{1-y}Cr_y)_2O_6$, $y=0.0033$, SBN:Cr] in the melt were grown by the Czochralski Method at the University of Osnabrück. All the crystals show natural facets and very homogeneous quality. Platelet-shaped samples with typical dimensions of $6\times6\times0.5$ mm^3 were cut with the polar c axis normal to the large plane and polished to optical quality. In order to erase the memory of any poling history and to enhance the relaxor properties,[20] the samples were annealed without electrodes at 893 K for 2 h and then slowly zero-field cooled (ZFC) to room temperature at a cooling rate of $\dot{T}=-0.004$ K/s. Vacuum deposition of copper and subsequent gold films were used to cover the major faces with electrodes. Prior to each measurement carried out on cooling, the samples were refreshed at 430 K for 0.5 h in order to ensure identical conditions for all measurements, and in order to eliminate possible memory of previous treatment. The dielectric susceptibility, $\chi=\chi'-i\chi''$, was measured using a Solartron 1260 impedance analyzer with a 1296 dielectric interface. The amplitude of the ac probing field was 500 V/m. The temperature was stabilized to within

TABLE I. Dielectric data for a SBN:Ce single crystal at $T=310$ K.

f	χ''_0	χ''_t	χ''_t/χ''_0	χ'_0	χ'_t	χ'_t/χ'_0
0.1 Hz	2200	825	0.4	18765	12960	0.7
10 kHz	1330	908	0.7	9865	8270	0.8

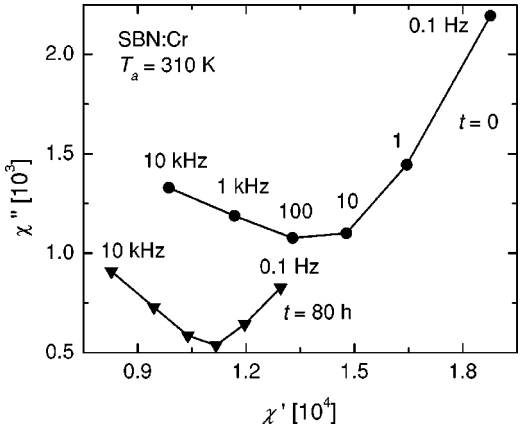

FIG. 2. Cole-Cole plots of nonaged (upper curve) and aged (80 h at 310 K) SBN:Cr. The lines are to guide the eyes.

±0.005 K with the help of a Lake Shore 340 temperature controller. Very precise temperature stabilization is required because of the very steep temperature dependence of χ in the vicinity of T_c.[10]

III. RESULTS AND DISCUSSION

Owing to the temperature dependence of the spontaneous polarization, a supposed rejuvenation effect in the SBN system was investigated first. To this end, the dielectric susceptibility measurement on the SBN:Cr single crystal at $10^{-1}\leqslant f\leqslant 10^4$ Hz on continuous ZFC from above T_c (rate $\dot{T}=-0.016$ K/s) has been interrupted by isothermal aging at $T_a=310$ K$<T_c$ for 80 h (curve 1 for $f=0.1$ and 10^4 Hz in Fig. 1). Similarly, as in lead-containing cubic relaxors,[13,14,21] a deep "hole is burnt" at T_a, indicating the domain state's approach to equilibrium by lower real and imaginary susceptibilities. Remarkably, the decrease in susceptibility during aging is much larger in the response tested at a lower frequency in comparison to that taken at a high-frequency one. This can convincingly be demonstrated by taking the ratio between the susceptibility components measured at a given frequency at $t=80$ h, χ_t, and the initial ones measured at $t=0$, χ_0, respectively. These quantities taken at two extreme frequencies 0.1 Hz and 10 kHz, and thus probing the system in two distinctively different dispersion regions,[22] are compared in Table I.

It is obvious that the aging effect is more pronounced in the imaginary part of susceptibility than in the real part. Very similar effects were reported for other systems as well.[13,21] More systematic inferences can be drawn from Fig. 2, where the data taken at other frequencies are displayed as two Cole-Cole-type plots, which clearly show two dispersion regions mentioned above by slopes with different signs. During isothermal aging both $\chi'(f)$ and $\chi''(f)$ decrease by about 20% to 50%, where the low-frequency branch referring to the irreversible polarization process[22] changes most drastically.

On further cooling to 295 K the hole is largely erased, i.e., the χ vs T curves approach the unaged reference ones (Fig. 1). This is at variance to the "cumulative" aging observed in SBN:La at $T=190$ K, where the cooling curve does

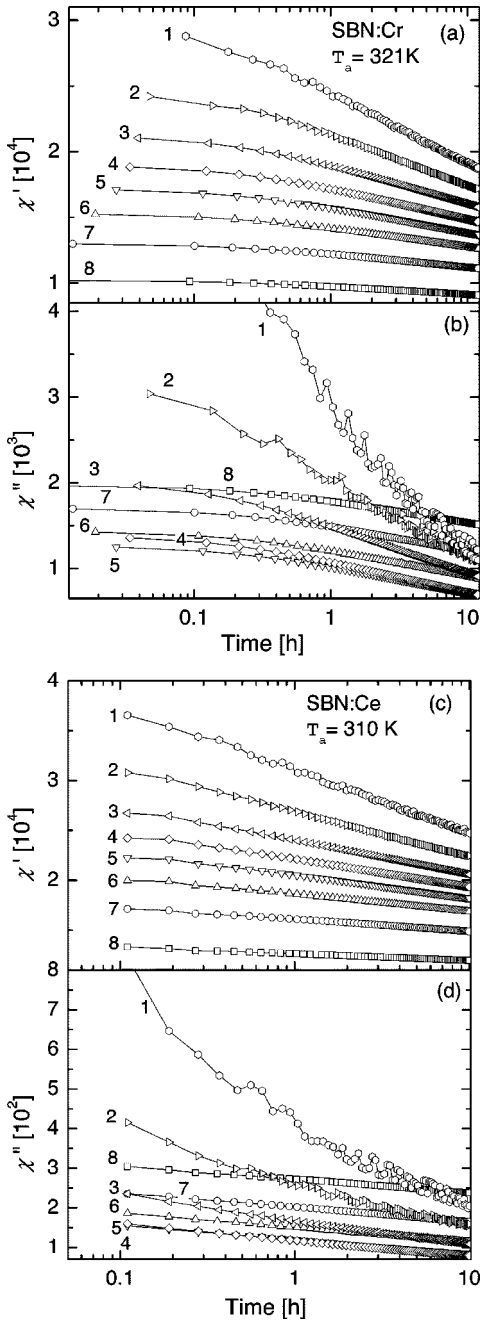

FIG. 3. Relaxation of the susceptibility components χ' (a, c) and χ'' (b, d) of SBN:Cr and SBN:Ce, respectively, measured after ZFC from 430 K vs time at $T=T_c-15$ K and frequencies $f=10^{-2}(1)$, $10^{-1}(2)$, $10^{0}(3)$, $10^{1}(4)$, $10^{2}(5)$, $10^{3}(6)$, $10^{4}(7)$, and 10^{5} Hz(8).

not reproduce the reference one.[14] However, upon successive reheating (curve 2) the hole is largely erased due to nonisothermal aging on cooling to below T_a. During the next monotonic cooling from $T=325$ K$<T_c$ (curve 3), a very smooth temperature dependence of χ is observed. The location of this run just between curves 1 and 2, respectively, is due to the partial refreshing occurring at temperatures close to T_c, however, this process is not as effective as in the initial refreshing one. Consequently, a cumulative decrease of χ in the run 3 is encountered as an example of the initial domain coarsening experienced at T_a.

Close to T_c the system encounters a chaotic regime, where the "equilibrium" domain state changes its structure as a function of T.[19] Such phenomena are well known from spin glasses[23] and confirm the mesoscopic spherical random bond RF (SRBRF) properties in cubic relaxors.[13,21] However, it is *a priori* not expected to occur in the metastable domain state of a 3*d* RFIM, whose average domain size should increase at any annealing step and thus give rise to cumulative changes of χ. Why does the system appear unrelaxed and reproduce the nonaged χ upon cooling? Probably, this is closely related to domain-wall evolution during annealing. On a temporal mesoscale, primarily the 180° walls will rearrange by optimizing the local free energy. These processes involve surface changes on head-to-head and tail-to-tail domain configurations, which tend to compensate volume RFs. Upon cooling, this local equilibrium becomes perturbed due to the T dependence of the spontaneous polarization, P. Hence, the domain-wall mobility, i.e., χ, tends to increase again as observed. Clearly, this hole-burning mechanism is no longer valid when cooling to $T\ll T_c$, where $P\approx$ constant.[14]

In order to reveal the temporal evolution of the axial susceptibility components, time dependences of χ' and χ'' were measured at selected T_a for both SBN:Cr and SBN:Ce. In the first series of experiments, each T_a was reached on ZFC from 430 K, where the sample had been refreshed for 0.5 h. Figure 3 presents the time dependences of χ measured at frequencies $10^{-2}\leqslant f\leqslant 10^{5}$ Hz during isothermal aging at $T_a=T_c-15$ K for SBN:Cr, $T_c=336$ K, [Figs. 3(a) and 3(b)], and SBN:Ce, $T_c=325$ K [Figs. 3(c) and 3(d)], respectively. It seems that both the real and imaginary parts of χ relax towards some equilibrium level, $\chi=\chi_\infty+\Delta\chi f(t)$, where $f(t)$ is a function varying from 1 to zero and the factor $\Delta\chi$ measures the amplitude of the time-dependent part of χ. In the observed time regime, all of our aging curves can be best fitted using the stretched exponential form

$$\chi(t)=\chi_\infty+\Delta\chi\,\exp(-t/\tau)^{\beta}, \tag{1}$$

while biexponential, inverse logarithmic, and power-law decay curves[24] prove to be less successful. Equation (1) con-

TABLE II. Fitting parameters referring to the relaxation of χ' and χ'' presented in Fig. 4, and the calculated autocorrelation time $\langle\tau\rangle$.

Data	χ^2	r^2	$\Delta\chi$	χ_∞	β	τ[h]	$\langle\tau\rangle$[h]
χ'	209	0.9998	8230±150	30050±130	0.514±0.007	9.6±0.5	18.3±1.2
χ''	8.7	0.9997	1048±18	913±13	0.496±0.009	5.0±0.2	10.2±0.6

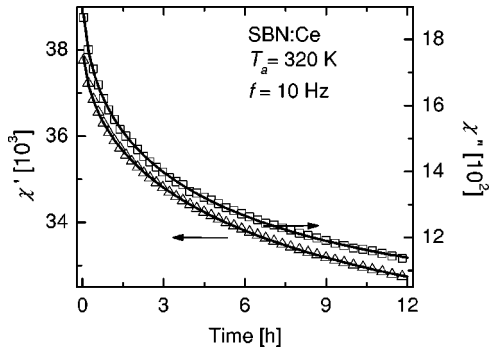

FIG. 4. Relaxation of the susceptibility of SBN:Ce measured after ZFC vs time at $T=320$ K and $f=10$ Hz and best fits to Eq. (1) (solid lines) with fitting parameters $\chi'_\infty=30050\pm130$, $\Delta\chi'=8230\pm150$, $\tau'=9.6\pm0.5$ h, $\beta'=0.514\pm0.007$, $(\chi^2)'=209$ and $(r^2)'=0.9998$ for χ', and $\chi''_\infty=916\pm13$, $\Delta\chi''=1048\pm18$, $\tau''=5.0\pm0.2$ h, $\beta''=0.496\pm0.009$, $(\chi^2)''=8.7$ and $(r^2)''=0.9997$ for χ'', respectively. For clarity only every second point is shown.

tains four adjustable parameters, χ_∞, $\Delta\chi$, the stretching exponent β and a characteristic relaxation time τ, which are listed in Table II together with the autocorrelation time $\langle\tau\rangle=(\tau/\beta)\Gamma(1/\beta)$.[25] It turns out that the values of fitting parameters practically do not depend on the time span chosen for the fitting procedure. This is why we finally decided to skip an additional free parameter t_0 as used by others[13,24] in order to take a possible delay into account. Equation (1) has been used to fit the real and imaginary components of χ data separately. As an example illustrating the quality of the fitting

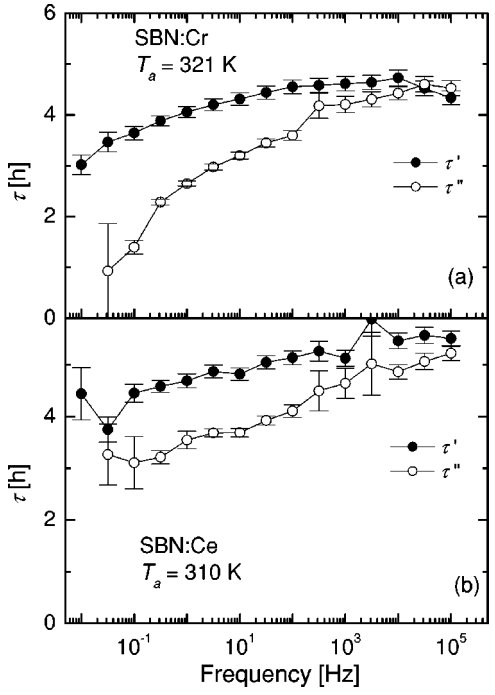

FIG. 5. Frequency dependences of the relaxation times τ' and τ'' (solid and open symbols, respectively) referring to the relaxation of χ' and χ'', respectively, as determined on SBN:Cr at $T_a=321$ K (a) and on SBN:Ce at $T_a=310$ K (b) after ZFC. The lines are to guide the eyes.

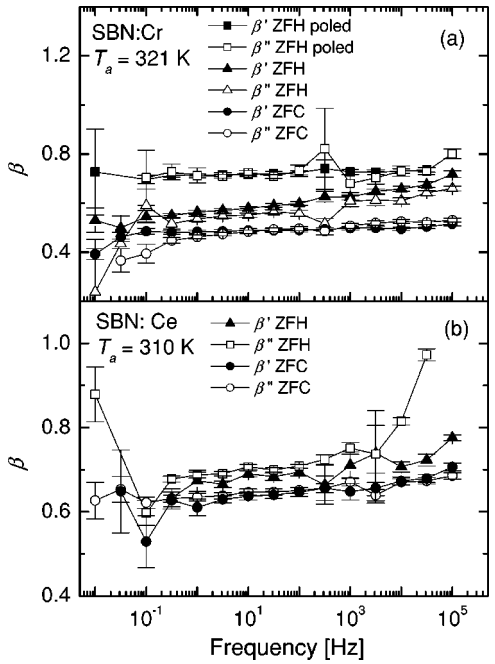

FIG. 6. Frequency dependences of the stretching exponent, β, as determined from the susceptibility relaxation of SBN:Cr (a) and SBN:Ce (b) (Fig. 3, see text). The lines are to guide the eyes.

procedure one may inspect Fig. 4, where the isotherms of a SBN:Ce sample taken at $T_a=320$ K and $f=10$ Hz after ZFC, and their fitting curves, are presented. Correlation coefficients $r^2=0.9998$ and 0.9997, respectively, were obtained and *chi*^{2} tests prove that the other functions listed above are definitely worse than Eq. (1).

Now we will discuss in more detail the behavior of the fitting parameters obtained from numerous isotherms. The relaxation rate is depicted by the characteristic relaxation time, τ. Frequency dependences of the relaxation times τ' and τ'' referring to the relaxation of χ' and χ'', respectively, are presented in Fig. 5. As is qualitatively clear by inspection of the isotherms presented in Fig. 3, the largest relaxation rates occur at the lowest frequencies, where the susceptibility is mainly controlled by creep.[22] This applies both to χ' and χ'' measured in both compounds. In addition, significant differences in the relaxation times, $\tau'>\tau''$, are observed in the low-frequency limit. Such a behavior seems to reflect different superpositions of individual contributions to the resultant χ' and χ'' responses, respectively. While χ' measured at a given frequency f_0 contains all the ingredients coming from $f\geqslant f_0$ (additivity of χ'), χ'' is mainly controlled by responses originating from frequencies adjacent to f_0. Consequently, τ' is a weighted average of a much larger number of constituent relaxation times than τ'', which results mainly from relaxators being active around f_0. Since the temporal relaxation is quicker for low f, then $\tau'-\tau''$ increases with the decreasing of f as observed in Fig. 5. Remarkably, in the case of SBN:Cr the difference $\tau'-\tau''$ is larger than in SBN:Ce. This difference gradually decreases as the frequency of the probing field is increased and practically vanishes for $f>10^4$ Hz. It is also worth stressing that the relaxation times (a few hours) are shorter than the experimental time scale of our

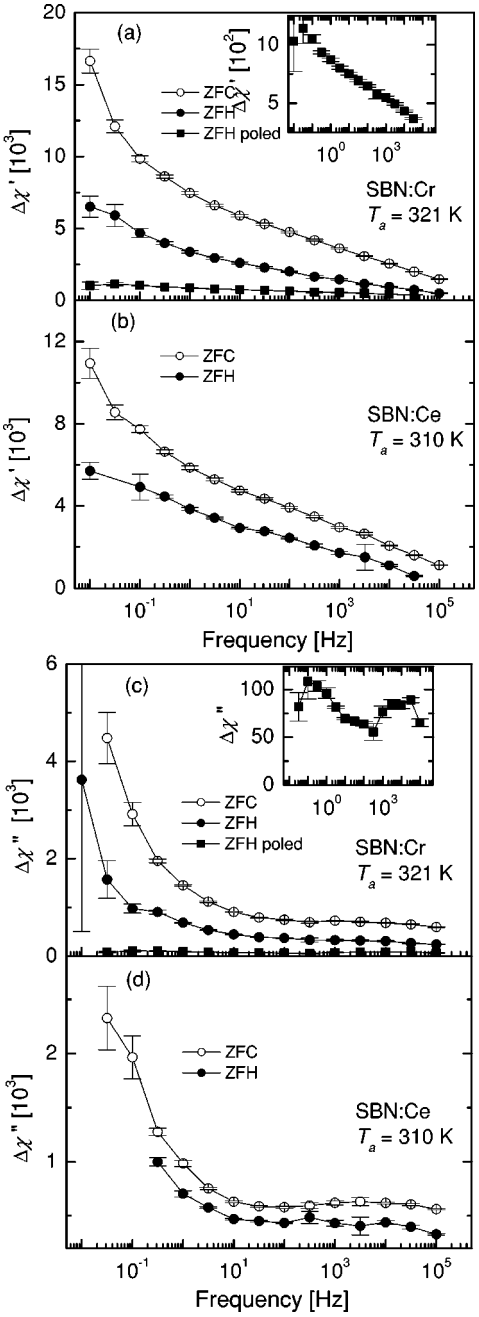

FIG. 7. Frequency dependences of the aging amplitude, $\Delta\chi$, as determined from the susceptibility relaxation of SBN:Cr (a, c) and SBN:Ce (b, d) (Fig. 3, see text). The lines are to guide the eyes. The insets to (a, c) show $\Delta\chi$ of poled SBN:Cr on expanded scales.

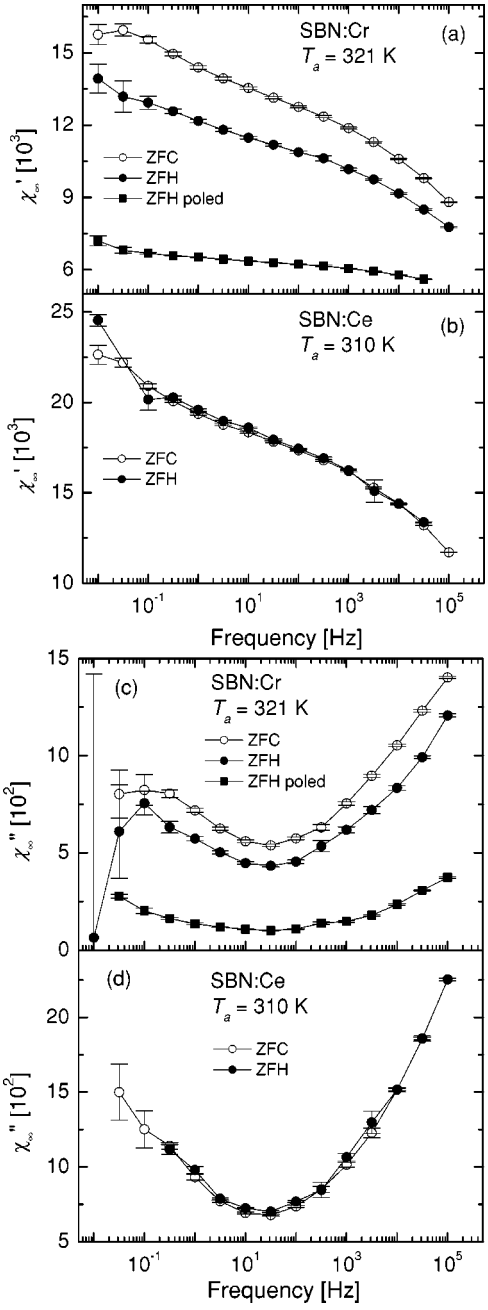

FIG. 8. Frequency dependences of the equilibrium values of susceptibility, χ_∞, as determined from the susceptibility relaxation of SBN:Cr (a, c) and SBN:Ce (b, d) (Fig. 3, see text). The lines are to guide the eyes.

measurements. Qualitatively similar behavior characterizes the relaxation when T_a is reached from below upon zero-field heating (ZFH) starting at $T=300$ K, where the sample had first been relaxed for 0.5 h. However, the relaxation times thus extracted are roughly two times longer than after ZFC from above T_c. In this case the system starts from a partly relaxed domain state and thus takes a longer time for final relaxation.

In contrast to the relaxation time, the stretching exponent β presents a quite different dependence on frequency. Within experimental errors it has values, $\beta \approx 0.3-0.6$, for both χ' and χ'' at nearly all frequencies, f (Fig. 6), where the values of β are generally smaller for the ZFC than for the ZFH procedures, respectively, and thus show a very clear influence of the sample history. The low values of β arising upon ZFC probably reflect the large size distribution in the domain state created during ZFC to T_a. In the case of ZFC to $T<T_a$ prior to ZFH to T_a the domains were subject to growth and gradual evolution towards a more uniform size distribution. This is why β measurably rises by about 0.1 (Fig. 6, open symbols). Consequently, after poling the exponent β increases to 0.72 ± 0.02 and remains almost frequency indepen-

dent as shown for poled SBN:Cr in Fig. 6(a). This seems to reflect a coarse domain structure remaining in the remanent poled state with some size distribution preventing the system from relaxing uniformly with $\beta=1$.

The components of the amplitude of aging relaxation, $\Delta\chi'$ and $\Delta\chi''$, display surprisingly large dispersive properties (Fig. 7). They drop quite rapidly in the low-frequency limit, $f<10$ Hz, and continue decreasing at higher frequencies, albeit at a smaller rate. The influence of the thermal history is imprinted again. The amplitudes are larger and decrease at a higher rate, if T_a is attained via ZFC as compared to the ZFH procedure. This is, again, a clear signature of a decreasing domain size dispersion when preaging in the latter mode. In the case of SBN:Cr, $\Delta\chi'$(ZFC) measured at 10^{-2} Hz is almost three times larger than $\Delta\chi'$(ZFH) [Fig. 7(a)]. After poling the SBN:Cr sample the dispersion of $\Delta\chi$ is substantially reduced as seen in Figs. 7(a) and 7(c), albeit it is still measurable as seen in the insets.

The most important conclusions can be drawn from Fig. 8, where the frequency dependences of χ_∞ are presented. The spectra of the equilibrated values of χ'_∞ and χ''_∞ are similar to the published nonequilibrated ones.[22] The real components, χ'_∞, display very broad dispersion steps at high frequencies, $f>10^5$ Hz, and points of inflection at $f\approx10$ Hz [Figs. 8(a) and 8(b)], while the losses have a well-defined minimum at $f\approx30$ Hz separating two different dispersion regions [Figs. 8(c) and 8(d)]. Poling strongly reduces the dispersive properties of both quantities. Here, a very striking difference between SBN:Cr and SBN:Ce systems is observed. While χ_∞ does not depend on history in the case of SBN:Ce [Figs. 8(b) and 8(d)], it shows a strong history dependence in SBN:Cr [Fig. 8(a) and 8(c)]. Very probably this must be attributed to the different electrochemical nature of Cr^{3+} and Ce^{3+} within the host SBN crystal.[17,18] Since Cr^{3+} replaces pentavalent Nb^{5+} on B sites it creates more oxygen vacancies than Ce^{3+}, which replaces Sr^{2+} and Ba^{2+} ions on A sites. Hence, Cr^{3+} is expected to give rise to a more complicated and finer grained charge disorder giving rise to a free-energy landscape with increased complexity. Here, we propose to follow the concept of different types of ergodicity breaking as postulated by Alberici *et al.*[24] SBN:Ce seems to reveal weak ergodicity breaking, such that the system is potentially able to visit the whole phase space during relaxation for very long times. In contrast, SBN:Cr is subject to true ergodicity breaking, where pseudoequilibrium states are separated by high barriers of the free-energy landscape, which are mutually unapproachable even after very long relaxation times.

Finally, a very instructive peculiarity: Having frequency dependences of χ_∞ and $\Delta\chi$, it is possible to reconstruct anticipated spectra for a nonaged sample. An example of such a reconstruction performed for a SBN:Ce sample is presented in Fig. 9, where the upper curve presents the frequency dependence of the sum $\chi'_\infty+\Delta\chi'$ based on the parameters originating from isothermal aging at $T_a=320$ K. For comparison, a direct experimental spectrum taken at the same temperature, after ZFC from 430 K, is displayed as well (open circles). These data interpolate between the anticipated unrelaxed and the final relaxed spectrum (Fig. 9).

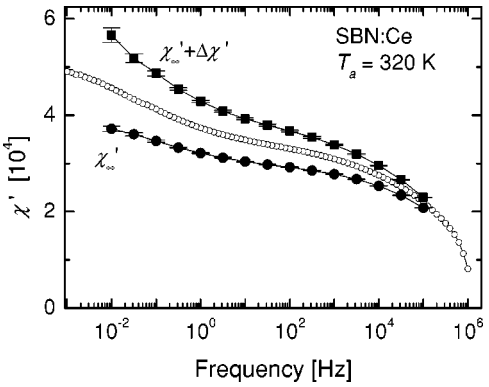

FIG. 9. Calculated unrelaxed and completely relaxed spectra, $\chi'_\infty+\Delta\chi'$ (solid squares) and χ'_∞ (solid circles), respectively, of SBN:Ce after ZFC to $T_a=320$ K together with a conventionally taken nominally unrelaxed spectrum, χ' (open circles).

IV. CONCLUSION

In summary, the uniaxial relaxor systems SBN:Cr and SBN:Ce display large aging effects when investigating the temporal dependences of dielectric response along the polar *c* axis. These effects are much larger than reported on systems, like lead magnoniobate-titanate (PMN-PT),[13] potassium lithium tantalate (KLT),[24] sodium bismuth titanate (NBT),[26] or rubidium dihydrogen phosphate (RDP).[27] Depending on the frequency range of the probing ac field, the aging effect is differently manifest. In the subhertz limit, where the dispersion of χ is due to the irreversible domain-wall creep processes,[22] aging is dominated by increasingly effective pinning of domain walls, thus decreasing the wall mobility. On the other hand, at $f>100$ Hz, where dispersion reflects segmental relaxation of the domain walls,[22] aging gives rise to an enhancement of local energy barriers and thus to a decrease of the dielectric response in addition to the effect of domain coarsening. Different kinds of doping in the SBN lattice give rise to weak and strong additional charge disorder, which leads to different types of ergodicity breaking. In the past, only sparse data on the aging of SBN can be found.[28,29] A systematic investigation and comprehensive analysis of the data obtained has been carried out in this paper.

ACKNOWLEDGMENTS

Financial support by DAAD and DFG (SPP "Strukturgradienten in Kristallen") is gratefully acknowledged.

[1] K. Uchino, Ferroelectrics **151**, 321 (1994).
[2] J.-Ph. Bouchaud, P. Doussineau, T. de Lacerda-Arôso, and A. Levelut, Eur. Phys. J. B **21**, 335 (2001), and references therein.
[3] A. Montanari and F. Ricci-Tersenghi, Phys. Rev. B **68**, 224429 (2003), and references therein.
[4] L. E. Cross, Ferroelectrics **151**, 305 (1994).
[5] A. Simon, J. Ravez, and M. Maglione, J. Phys.: Condens. Matter **16**, 963 (2004).
[6] V. Westphal, W. Kleemann, and M. D. Glinchuk, Phys. Rev. Lett. **68**, 847 (1992).
[7] W. Kleemann, Int. J. Mod. Phys. B **7**, 2469 (1993).
[8] W. Kleemann, J. Non-Cryst. Solids **307–310**, 66 (2002).
[9] R. Pirc and R. Blinc, Phys. Rev. B **60**, 13470 (1999).
[10] W. Kleemann, J. Dec, P. Lehnen, Th. Woike, and R. Pankrath, in *Fundamental Physics of Ferroelectrics 2000*, edited by R. E. Cohen, AIP Conf. Proc. No. 535, p. 26 (AIP, New York, 2000).
[11] W. Kleemann, J. Dec, P. Lehnen, R. Blinc, B. Zalar, and R. Pankrath, Europhys. Lett. **57**, 14 (2002).
[12] P. Lehnen, W. Kleemann, Th. Woike, and R. Pankrath, Phys. Rev. B **64**, 224109 (2001).
[13] O. Kircher and R. Böhmer, Eur. Phys. J. B **26**, 329 (2002).
[14] M. B. Weissman, E. V. Colla, and L. K. Chao, in *Fundamental Physics of Ferroelectrics 2003*, edited by P. K. Davies and D. J. Singh, AIP Conf. Proc. No. 677, p. 33 (AIP, New York, 2003).
[15] K. Jonason, P. Nordblad, E. Vincent, J. Hammann, and J.-P. Bouchaud, Eur. Phys. J. B **13**, 99 (2000).
[16] P. Doussineau, T. de Lacerda Arôso, and A. Levelut, Eur. Phys. J. B **16**, 455 (2000).
[17] M. Gao, R. Pankrath, S. Kapphan, and V. Vikhnin, Appl. Phys. B: Lasers Opt. **68**, 849 (1999), and references therein.
[18] J. Wingbermühle, M. Meyer, O. F. Schirmer, R. Pankrath, and R. K. Kremer, J. Phys.: Condens. Matter **12**, 4277 (2000).
[19] J. Villain, Phys. Rev. Lett. **52**, 1543 (1984).
[20] R. Guo, S. Bhalla, G. Burns, and F. H. Dacol, Ferroelectrics **93**, 397 (1989).
[21] E. V. Colla, L. K. Chao, M. B. Weissman, and D. D. Viehland, Phys. Rev. Lett. **85**, 3033 (2000).
[22] W. Kleemann, J. Dec, S. Miga, Th. Woike, and R. Pankrath, Phys. Rev. B **65**, 220101 (2002).
[23] T. Jonsson, K. Jonason, and P. Nordblad, Phys. Rev. B **59**, 9402 (1999).
[24] F. Alberici, P. Doussineau, and A. Levelut, J. Phys. I **7**, 329 (1997).
[25] K. Binder and J. D. Reger, Adv. Phys. **41**, 547 (1992).
[26] K. Roleder, J. Suchanicz, and A. Kania, Ferroelectrics **89**, 1 (1989).
[27] V. Mueller and Ya. Shchur, Europhys. Lett. **65**, 137 (2004).
[28] T. W. Cline and L. E. Cross, J. Appl. Phys. **49**, 4298 (1978).
[29] G. Borchhardt, J. von Cieminski, and G. Schmidt, Phys. Status Solidi A **59**, 749 (1980).